# $\alpha$-$Gd_2S_3$-type structure in $In_2O_3$: Experiments and theoretical confirmation of a high-pressure polymorph in sesquioxide

Hitoshi Yusa*
*Advanced Nano Materials Laboratory, National Institute for Materials Science, 1-1 Namiki, Tsukuba 305-0044, Japan*

Taku Tsuchiya and Jun Tsuchiya
*Geodynamics Research Center, Ehime University, 2-5 Bunkyo-cho, Matsuyama 790-8577, Japan*

Nagayoshi Sata
*Japan Agency for Marine-Earth Science and Technology, 2-15 Natsushima-cho, Yokosuka 237-0061, Japan*

Yasuo Ohishi
*Japan Synchrotron Radiation Research Institute, 1-1-1 Kouto, Sayo-cho 679-5198, Japan*
(Received 30 June 2008; revised manuscript received 19 August 2008; published 24 September 2008)

A high-pressure phase, orthorhombic $\alpha$-$Gd_2S_3$ type, was found in $In_2O_3$ as a post-$Rh_2O_3$(II) phase at pressures over 40 GPa by using an *in situ* x-ray diffraction method. This structure is composed of unusual sevenfold and eightfold coordinated cations, which has not been predicted for any sesquioxides to date. Compared with the known post-$Rh_2O_3$(II) transition to the $CaIrO_3$ structure, this transition to $\alpha$-$Gd_2S_3$ yields a considerable volume change. Density functional lattice energy calculations also show that the transition to $\alpha$-$Gd_2S_3$ is more favorable than the transition to $CaIrO_3$ in $In_2O_3$.

DOI: 10.1103/PhysRevB.78.092107 PACS number(s): 61.50.Ks, 61.05.cp, 61.50.Ah, 62.50.−p

Searching for a denser structure than corundum in sesquioxides is attractive to material scientists seeking hard materials. Since the structural transformation from corundum to the $Rh_2O_3$(II) (Ref. 1) structure was reported in $Al_2O_3$,[2,3] the postcorundum phases in various sesquioxides [(i.e., $Fe_2O_3$,[4–7] $Cr_2O_3$,[8] $Ga_2O_3$,[9,10] and $In_2O_3$ (Ref. 10)] have been actively studied both experimentally and theoretically. In those investigations, $Rh_2O_3$(II) structure was identified as the postcorundum phase in $Fe_2O_3$, $Ga_2O_3$, $Cr_2O_3$, and $In_2O_3$ by using *in situ* x-ray diffraction methods and a laser heated diamond anvil cell (LHDAC). This structure is similar to the corundum structure except for a different stacking of octahedral layers.[1] Further structural evolution from $Rh_2O_3$(II) phases to $CaIrO_3$-type (space group *Cmcm*) phases was reported in $Al_2O_3$,[11,12] $Fe_2O_3$,[13] and $Ga_2O_3$ (Ref. 9) at high pressures of 130, 60, and 164 GPa, respectively. The $CaIrO_3$ structure is identical to the $MgSiO_3$ postperovskite phase, which is expected to be stable at the pressure (~120 GPa) close to the base of the Earth's lower mantle.[14,15] The $CaIrO_3$-type structure consists of both sixfold and eightfold coordinated cation sites, of which the sixfold octahedra share the edges to make an octahedral chain. One of the 3*d* transition-metal sesquioxides, $\alpha$-$Mn_2O_3$ (bixbyite, *C*-type rare-earth sesquioxide structure, denoted as *C*-RES hereafter), which is composed of rather distorted oxygen coordinated octahedra due to Jahn-Teller (JT) distortion at atmospheric pressure,[16] also undergoes a phase transition to the $CaIrO_3$ structure at 27–38 GPa.[17] Interestingly, $\alpha$-$Mn_2O_3$ directly transforms into the $CaIrO_3$ structure with no intermediate corundum or $Rh_2O_3$(II) structure, accompanied by suppression of the JT distortion. These reports suggest that the sixfold octahedron would be very rigid under high pressure in sesquioxides. No further high-pressure phase transition to structures with the cation coordination higher than seven has yet been discovered in those compounds. Here, we report on an indium sesquioxide polymorph composed of sevenfold and eightfold coordinations. Structures and phase relations were also examined theoretically by density functional computations.

High-purity indium oxide powder (Aldrich, 99.999% pure; *C*-RES) was used for the high-pressure experiments. The high-pressure x-ray powder-diffraction experiments were carried out at BL10XU in SPring-8 in the same manner as our previous study.[10,18] We targeted a pressure range of more than 30 GPa in order to explore the post-$Rh_2O_3$(II) phase, since we found a transition to the $Rh_2O_3$(II) structure below 20 GPa as a postcorundum phase change in a previous study.[10] In the first run, the sample was compressed up to 51 GPa. The x-ray profile of the compressed sample first exhibits an amorphouslike halo pattern [Fig. 1(a)]. Then, the laser heated the sample at 2000–2500 K for 15 min. After laser heating, the halo changed to many sharp peaks which were from a crystalline phase [Fig. 1(c)]. The pressure dropped to 45 GPa during heating. The new diffraction pattern is obviously different from that of the $Rh_2O_3$(II) phase. After releasing the pressure, these diffraction peaks changed to broad peaks that could be assigned to be the corundum structure [Fig. 1(e)].

We searched for a possible high-pressure structure on the basis of the phase transformation systematics in sesquioxides. Contrary to the initial expectation, the present diffraction pattern completely disagrees with that expected from the $CaIrO_3$ structure, which had been already found as the post-$Rh_2O_3$(II) phase in several sesquioxides as mentioned above. Since the $In_2O_3$ forms the six-oxygen coordinated structure under low-pressure conditions, the plausible higher oxygen-coordinated phases, *B*-RES and *A*-RES, which are composed of six- and seven-type, and seven-type oxygen coordinations,[19] respectively, were also examined as possible matches with the present diffraction pattern. However, we

 ©2008 The American Physical Society

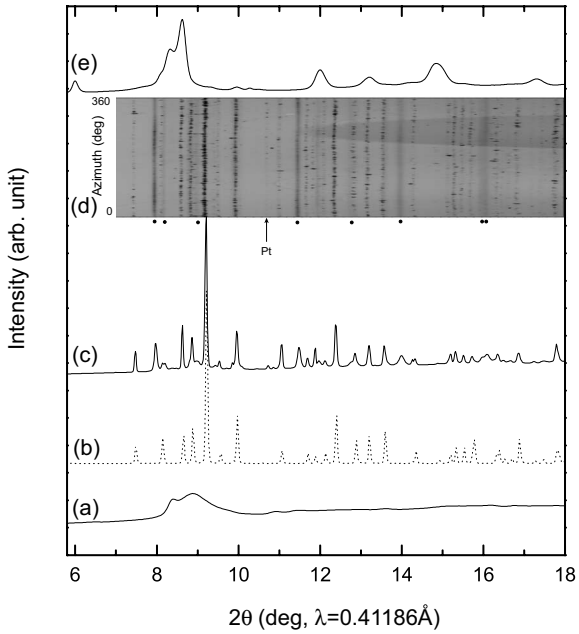


FIG. 1. X-ray powder-diffraction profiles obtained by IP: (a) at 51 GPa before heating; (c) at 45 GPa after laser heating; (e) after decompression. Raw 2D image (azimuth vs $2\theta$) (d) is shown for comparison with the profile of (c). The reflections marked with small dots are not identified. An arrow indicates the position of platinum's reflection. A simulated profile (b) based on $\alpha$-$Gd_2S_3$ structure is shown for comparison.

could not give indices to the present profile based on their structures. Therefore, we tried to search for an adaptable unit cell by using computer program based indexing with the dichotomy method (DICVOL04).[20] Input of all of the observed 39 peaks in the program did not propose any candidates for the unit cell. However, if one carefully looks at the two-dimensional (2D) pattern [Fig. 1(d)], one can realize that several broad diffraction lines appear around 8.0°, 8.2°, 9.0°, 11.5°, 12.8°, 14.0°, 16.0°, and 16.1°, which might be derived from a metastable phase being formed in the colder part at the contact surface with diamond anvils.[21] Since the broad peaks often appear in the same kind of experiments,[9,22] we eliminated them from the input data to search for the unit cell. Then, we successfully determined an orthorhombic unit cell with $a=5.473(1)$ Å, $b=3.003(1)$ Å, and $c=11.618(3)$ Å by using 31 peaks. Considering the volume contraction from the $Rh_2O_3$(II) phase, four formula units ($Z=4$) in the unit cell are reasonable for the density (9.653 $g/cm^3$). Miller indices can be assigned to all peaks within acceptable errors.[18] Reflection conditions derived from the assigned reflections were $k+l=2n$ for $0kl$, $h=2n$ for $hk0$ and $h00$, and $l=2n$ for $00l$, affording possible space groups of $Pnma$ and $Pn2_1a$.[23] As described above, we could not find any structure related to those space groups in the known sesquioxide structures. Through further investigation, however, we noticed the rare-earth sesquisulfide structures. There are eight crystal structures, e.g., $\alpha$, $\beta$, $\gamma$, $\delta$, $\epsilon$, $\sigma$, $\eta$, and $\varphi$ phase, reported for rare-earth sesquisulfide.[24] Although the $\alpha$- and $\eta$-type structures belong to the $Pnma$ space group, the relationship of the cell lengths ($b/a\sim0.6$ and $c/a\sim2.2$) allows only the $\alpha$ structure, which is represented by $Gd_2S_3$.[25]

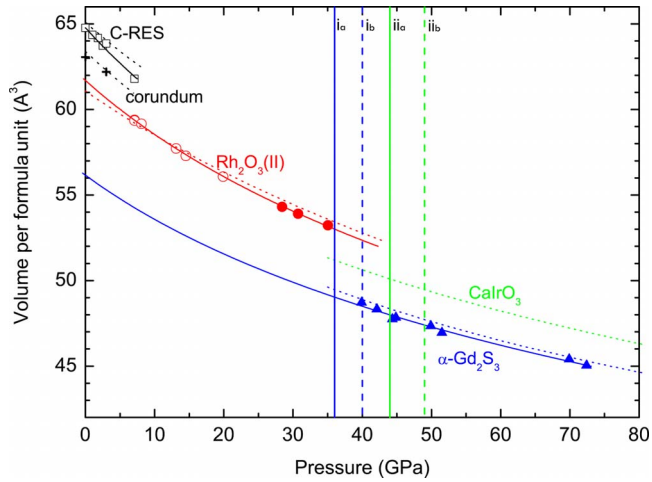


FIG. 2. (Color online) $P$-$V$ data of $C$-RES (squares), corundum (crosses), $Rh_2O_3$(II) (circles), and $\alpha$-$Gd_2S_3$ (triangles). Crosses and open symbols are our previous results (Ref. 10). All volume data are normalized per formula unit. The compression curve (solid lines) was obtained by fitting the data to the $B$-$M$ EoS. $P$-$V$ curves by DFT-LDA (dotted lines) are shown together for comparison (Ref. 10). Vertical solid lines ($i_a$ and $ii_a$) and broken lines ($i_b$ and $ii_b$) indicate the pressures of enthalpy crossover points (Fig. 3) by LDA and GGA computations, respectively.

Regarding anion coordination around metal atoms, the $\alpha$-$Gd_2S_3$ structure has seven and eight sulfur coordinations, which are higher than the oxygen coordination in $A$-RES sesquioxide structures. Furthermore, the volume contraction from $Rh_2O_3$(II) to $\alpha$-$Gd_2S_3$ is estimated to be 7%–8%, which is significantly larger than the 2%–3% in the known $Rh_2O_3$(II)$-CaIrO_3$ transitions,[9,11,13] indicating that this structure is much more favorable to the high-pressure phase than the $CaIrO_3$ structure. Therefore, we concluded that the high-pressure structure coincides with the $\alpha$-$Gd_2S_3$ structure. We then repeated the high $P$, $T$ experiments in the wide pressure range between 28 and 72 GPa to elucidate the stability range of the new phase more precisely. The data are plotted in Fig. 2. The $Rh_2O_3$(II) phase was clearly observed up to 35.4 GPa. In the subsequent runs around 40–42 GPa, the transient process to the $\alpha$-$Gd_2S_3$ phase was observed. Therefore, the transition pressure can be estimated to be close to 40 GPa at high temperature. In contrast, at 70–72 GPa, the $\alpha$-$Gd_2S_3$ phase coexisted with an unidentified phase, suggesting a further high-pressure phase change.

Computations were performed within the framework of density functinoal theory (DFT) with the local density approximation (LDA) and the generalized gradient approximation (GGA) to $\alpha$-$Gd_2S_3$-type phase in the phase sequence of indium sesquioxide. Details about the total-energy calculations and pseudopotentials used here are reported in Ref. 18. The calculated relative enthalpy of $\alpha$-$Gd_2S_3$ with respect to corundum-type $In_2O_3$ is indicated in Fig. 3 along with the enthalpies of other polymorphs, $C$-RES, $Rh_2O_3$(II), and $CaIrO_3$. In our previous study of phase transformations in $Ga_2O_3$, the $Rh_2O_3$(II) phase was confirmed to be the postcorundum phase as in $In_2O_3$, which was followed by the

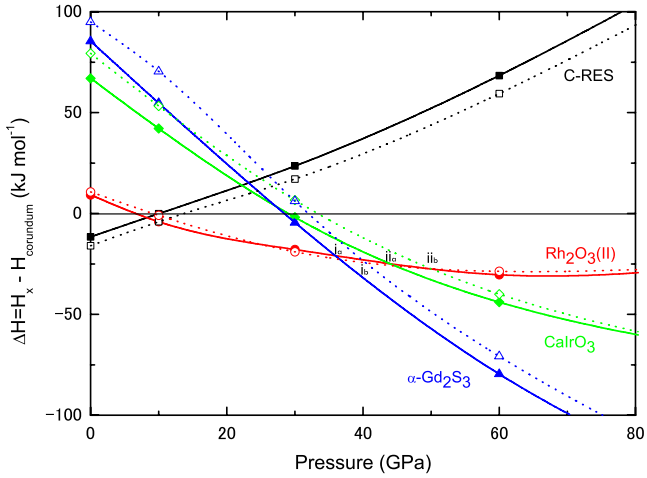


FIG. 3. (Color online) Enthalpy differences relative to corundum for *C*-RES (squares), $Rh_2O_3$(II) (circles), $\alpha$-$Gd_2S_3$ (triangles), and $CaIrO_3$ (diamonds) in $In_2O_3$. Solid lines and dotted lines indicate LDA and GGA computation results, respectively.

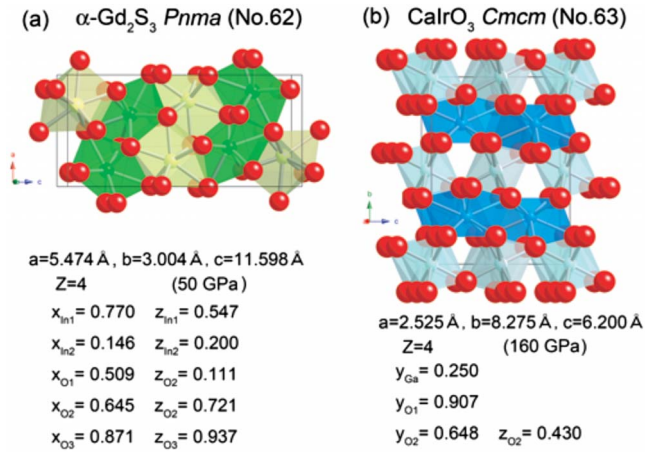


FIG. 4. (Color online) Crystal structures of (a) $\alpha$-$Gd_2S_3$ in $In_2O_3$ and (b) $CaIrO_3$ in $Ga_2O_3$. Large spheres are oxygen. Small spheres in (a) and (b) are indium and gallium, respectively. Deep color polyhedra represent bicapped trigonal prism.

$CaIrO_3$ phase. In Fig. 3, we find the enthalpy crossovers related to the $Rh_2O_3$(II)$-\alpha$-$Gd_2S_3$($i_a$ and $i_b$) and $Rh_2O_3$(II) $-CaIrO_3$($ii_a$ and $ii_b$) transitions, which locate around 36–40 GPa and 44–49 GPa, respectively. Enthalpy of the $CaIrO_3$ phase is therefore completely eclipsed by the enthalpies of $Rh_2O_3$(II) and $\alpha$-$Gd_2S_3$, meaning that $CaIrO_3$ has no own stability field at least at 0 K conditions. This suggests that in contrast to $Al_2O_3$ and $Ga_2O_3$, the transition from $Rh_2O_3$(II) to $CaIrO_3$ is thermodynamically hindered by the stabilization of $\alpha$-$Gd_2S_3$ in the case of $In_2O_3$.

Due to the lack of uniformity in intensity in the spotty diffraction pattern, it is difficult to determine the atomic coordinates of the $\alpha$-$Gd_2S_3$-type phase by Rietveld analysis. Instead, we compared the measured x-ray diffraction profile with the intensity based on the atomic coordinates optimized by DFT-LDA [Fig. 1(b)]. The observed intensity is in good agreement with the simulation except for several broad peaks mentioned above. The crystallographic view of the $\alpha$-$Gd_2S_3$-type phase based on the atomic coordinates is indicated in Fig. 4. The structure consists of two kinds of indium sites, coordinated by seven and eight oxygen atoms. The coordination polyhedra of $InO_7$ and $InO_8$ form monocapped and bicapped trigonal prisms, respectively. A capped trigonal prism arrangement is common for rare-earth oxides, sulfides, selenides, and tellurides.[24] Indeed, *B*– and *A*-RESs are partially or fully composed of monocapped trigonal prisms. However, there have been no reports on any high oxygen-coordinated structures composed of both monocapped and bicapped trigonal prisms in the sesquioxides,[24] suggesting that the $\alpha$-$Gd_2S_3$-type $In_2O_3$ is one of the densest phases of the known sesquioxides.

By fitting the *P*-*V* data to the Birch-Murnaghan equation of state (*B*-*M* EoS), the bulk modulus ($B_0$) was calculated to be $174 \pm 15$ GPa with the pressure derivative ($B_0$) fixed to 5.4, which is obtained from DFT-LDA calculation. We could not directly measure the $V_0$ of the $\alpha$-$Gd_2S_3$ phase because of the unquenchable behavior down to the ambient pressure. The $V_0$ can be approximated by extrapolation using *B*-*M* EoS (Fig. 2). The volume change from the $Rh_2O_3$(II) structure in $In_2O_3$, $\Delta V_0 = (V_{Rh_2O_3(II)} - V_{\alpha\text{-}Gd_2S_3})/V_{Rh_2O_3(II)}$ is calculated to be 8.3%, which is considerably larger than the 2.5% in the case of the post-$Rh_2O_3$(II) transition to $CaIrO_3$ in $Ga_2O_3$, $\Delta V_0 = (V_{Rh_2O_3(II)} - V_{CaIrO_3})/V_{CaIrO_3}$.[9] At the transition pressure, the large volume difference in $In_2O_3$ still remains, which is 7.6% at 36 GPa. The volume difference between the $Rh_2O_3$(II) and $CaIrO_3$ structures in other sesquioxides also exhibits 2.8%–3.0% at their transition pressures.[11,13] These volume changes associated with two types of post-$Rh_2O_3$(II) phase change can be explained by referring to the cation-oxygen distances and the effective coordination number (ECoN) (Refs. 26 and 27) of the coordination polyhedra in each structure (Table I). The ECoN is defined as

$$\mathrm{ECoN} = \sum_i w_i, \tag{1}$$

where

$$w_i = \exp[1 - (l_i/l_{av})^6] \tag{2}$$

is called the "bond weight" of the *i*th bond. In Eq. (2), $l_{av}$ represents a weighted average bond length defined as

TABLE I. Classical coordination numbers (CN) and effective coordination numbers (ECoN) of oxygen-coordinated polyhedra in sesquioxides.

| Compound | Phase | Polyhedron | CN | ECoN |
|---|---|---|---|---|
| $Al_2O_3$ | $CaIrO_3$ | OCT[a] | 6 | 5.95 |
| | | BTP[b] | 8 | 6.60 |
| $Ga_2O_3$ | $CaIrO_3$ | OCT | 6 | 5.89 |
| | | BTP | 8 | 6.79 |
| $In_2O_3$ | $\alpha$-$Gd_2S_3$ | MTP[c] | 7 | 6.77 |
| | | BTP | 8 | 7.71 |

[a]Octahedron.
[b]Bicapped trigonal prism.
[c]Monocapped trigonal prism.

$$l_{\mathrm{av}} = \frac{\sum_i l_i \exp[1-(l_i/l_{\min})^6]}{\sum_i \exp[1-(l_i/l_{\min})^6]}, \quad (3)$$

where $l_{\min}$ is the shortest bond length in the coordination polyhedron. The $CaIrO_3$ structure consists of two types of oxygen-coordinated polyhedra, octahedra with smaller volume, and an eightfold coordinated bicapped trigonal prisms with larger volume. Compared with the $Rh_2O_3$(II) structure, where all cations are in the octahedral coordination, the oxygen coordination in $CaIrO_3$ in part apparently increases from six to eight. Contrary to the small variation in Al-O and Ga-O distances within 2%–3% in octahedra,[9,11] the variations in the bicapped prism are significantly large (ca. 10%). This irregularity in terms of the cation-oxygen distances in the bicapped prism reduces the coordination number of 8 to ECoNs of 6.60–6.79. Therefore, the total volume does not so largely decrease across the transition from $Rh_2O_3$(II) to $CaIrO_3$ as expected from the apparent increase in the coordination number. In contrast, the In-O distances in both the monocapped and bicapped trigonal prism of $\alpha$-$Gd_2S_3$ structures exhibit only a little variety. The ECoNs of these polyhedra are then estimated to be 6.77 and 7.71, respectively, which are very close to the apparent coordination numbers. This appears to be a primary reason for the large volume reduction, which is feasible in the $\alpha$-$Gd_2S_3$. Hence, in terms of density, the $CaIrO_3$ phase, which is the postperovskite phase in some ternary compounds, is thought to be a transient phase in the high-pressure polymorphs in sesquioxides.

In the present study, we discovered a phase transformation from the $Rh_2O_3$(II) structure to the $\alpha$-$Gd_2S_3$ structure in sesquioxides. Despite the extensive theoretical and experimental studies investigating the high-pressure sesquioxide transition sequences to date, no research had ever noticed the stabilization of this sesquisulfide structure in any sesquioxide. As well as the $CaIrO_3$ structure, the $\alpha$-$Gd_2S_3$ structure is also recognized as a post-$Rh_2O_3$(II) structure. If the $\alpha$-$Gd_2S_3$ structure would be found as a recovery product in some sesquioxide or ternary compounds, it would be one of the candidates for dense and hard materials. The results open a research field in crystallography, materials science, and earth science to understand the systematics of the structural evolution of oxides under pressure. For example, an exploratory study of the $\alpha$-$Gd_2S_3$ structure under ultrahigh pressure would be of interest for other sesquioxides[28] and also for $ABO_3$-type ternary compounds.

## ACKNOWLEDGMENTS

The synchrotron-radiation experiments were performed at the BL-10XU in SPring-8 with the approval of JASRI. H.Y. acknowledges support from NIMS Competitive Research Funds. T.T. and J.T. acknowledge support from Ehime University Project Fund and Grant-in-Aid for Scientific Research from the JSPS.

*yusa.hitoshi@nims.go.jp

[1] R. D. Shannon and C. T. Prewitt, J. Solid State Chem. **2**, 134 (1970).
[2] N. Funamori and R. Jeanloz, Science **278**, 1109 (1997).
[3] J. F. Lin, O. Degtyareva, C. T. Prewitt, P. Dera, N. Sata, E. Gregoryanz, H. K. Mao, and R. J. Hemley, Nat. Mater. **3**, 389 (2004).
[4] M. P. Pasternak, G. K. Rozenberg, G. Y. Machavariani, O. Naaman, R. D. Taylor, and R. Jeanloz, Phys. Rev. Lett. **82**, 4663 (1999).
[5] G. K. Rozenberg, L. S. Dubrovinsky, M. P. Pasternak, O. Naaman, T. Le Bihan, and R. Ahuja, Phys. Rev. B **65**, 064112 (2002).
[6] S. Ono, T. Kikegawa, and Y. Ohishi, J. Phys. Chem. Solids **65**, 1527 (2004).
[7] S. Ono, K. Funakoshi, Y. Ohishi, and E. Takahashi, J. Phys.: Condens. Matter **17**, 269 (2005).
[8] S.-H. Shim, T. S. Duffy, R. Jeanloz, C.-S. Yoo, and V. Iota, Phys. Rev. B **69**, 144107 (2004).
[9] T. Tsuchiya, H. Yusa, and J. Tsuchiya, Phys. Rev. B **76**, 174108 (2007).
[10] H. Yusa, T. Tsuchiya, N. Sata, and Y. Ohishi, Phys. Rev. B **77**, 064107 (2008).
[11] J. Tsuchiya, T. Tsuchiya, and R. M. Wentzcovitch, Phys. Rev. B **72**, 020103(R) (2005).
[12] S. Ono, A. Oganov, T. Koyama, and H. Shimizu, Earth Planet. Sci. Lett. **246**, 326 (2006).
[13] S. Ono and Y. Ohishi, J. Phys. Chem. Solids **66**, 1714 (2005).
[14] M. Murakami, K. Hirose, K. Kuwayama, N. Sata, and Y. Ohishi, Science **304**, 855 (2004).
[15] T. Tsuchiya, J. Tsuchiya, K. Umemoto, and R. M. Wentzcovitch, Earth Planet. Sci. Lett. **224**, 241 (2004).
[16] S. Geller, Acta Crystallogr., Sect. B: Struct. Crystallogr. Cryst. Chem. **27**, 821 (1971).
[17] J. Santillan, S.-H. Shim, G. Shen, and V. B. Prakapenka, Geophys. Res. Lett. **33**, L15307 (2006).
[18] See EPAPS Document No.E-PRBMDO-78-060833 for details about the high-pressure experiments and total energy calculations, and the result of *d* value refinement. For more information on EPAPS, see http://www.aip.org/pubservs/epaps.html.
[19] A. F. Wells, *Structural Inorganic Chemistry*, 5th ed. (Clarendon, Oxford, 1984).
[20] A. Boultif and D. Louer, J. Appl. Crystallogr. **37**, 724 (2004).
[21] H. Morishima and H. Yusa, J. Appl. Phys. **83**, 4572 (1998).
[22] H. Yusa, N. Sata, and Y. Ohishi, Am. Mineral. **92**, 2007 (2008).
[23] T. Hahn, *International Table for Crystallography*, 5th ed. (Kluwer, Dordrecht, 2002).
[24] J. Flahaut, *Handbook on the Physics and Chemistry of Rare Earths* (North-Holland, Amsterdam, 1979), Vol. 4, pp. 1–88.
[25] C. T. Prewitt and A. W. Sleight, Inorg. Chem. **7**, 1090 (1968).
[26] R. Hoppe, Z. Kristallogr. **150**, 23 (1979).
[27] K. Momma and F. Izumi, IUCR Newsl. **7**, 106 (2006), a program VESTA performs calculations of ECoN.
[28] H. Yusa, T. Tsuchiya, N. Sata, and Y. Ohishi (unpublished).